Searching for reversible hydrogen storage materials

*Young Whan Cho and Jae-Hyeok Shim
Nano-Materials Research Center, Korea Institute of Science and Technology, Seoul 136-791, Republic of Korea
e-mail) oze@kist.re.kr

Abstract

Some complex metal hydrides such as alkali and alkali-earth metal aluminium hydrides, borohydrides and amides have high hydrogen contents of more than 5 % but only few of them have been studied so far as potential reversible hydrogen storage materials. Ti-catalyzed $NaAlH_4$ and a mixture of $LiNH_2$ and LiH or MgH_2 are the only cases which show reproducible dehydrogenation/hydrogenation cycles below 200 ℃ with ultimate hydrogen storage capacities of more than 5 %. We are carrying out series of experimental works on synthesizing Li- and Mg-alanates as well as zinc borohydride by mechanochemical reaction and characterizing their thermal decomposition behaviour with and without appropriate catalysts. Thermodynamic calculations on the destabilization of high temperature binary hydrides and complex metal hydrides are also being actively carried out in our group. Some of the results of our recent works on Li and Mg alanates as well as zinc borohydride will be presented together with some promising destabilized systems, such as MgH_2-Si and $LiBH_4$-MgH_2.

Key words: hydrogen storage materials, reversible metal hydride, alanate, borohydride, catalyst

1. Introduction

For on-board applications, it is vital to develop compact, light, safe, and affordable hydrogen storage systems. So far, compressed gas and cryogenic liquid hydrogen storage systems are most intensively developed but both are not regarded as ultimate solutions for fuel cell automobile applications due to safety concerns, volumetric constraints and energy losses. Solid hydrogen storage based on various hydrides such as interstitial, ionic, and covalent metal hydrides, is considered as an alternative. Most interstitial (or metallic) hydrides, such as $LaNi_5H_6$, $FeTiH_2$, and TiV_2H_4, absorb and desorb hydrogen readily around room temperature

but have insufficient hydrogen storage capacity (< 2 %) for on-board applications. Some of the lightest elements in the periodic table, for example lithium and sodium, form stable ionic compounds with hydrogen. Although the hydrogen content reaches values of up to 12.6 % for LiH, such compounds desorb hydrogen only at very high temperatures (> 600 ℃). MgH_2 is a well known covalent hydride with 7.6 % hydrogen storage capacity but decomposes at 285 ℃ for 1 bar hydrogen. There are a few other reversible hydrides with high theoretical hydrogen storage capacity above 5 %, and Ti-catalyzed $NaAlH_4$ is among them [1].

Despite decades of extensive research efforts, however, no material has been found yet, which has the combination of high gravimetric hydrogen density, adequate hydrogen dissociation energetics and reliability. An increasing demand for high density hydrogen sources applicable to fuel cells for automobile applications has recently stimulated research on complex hydrides of light elements such as aluminum and boron, which have very high theoretical hydrogen storage capacities up to 11%. However, very little is known on most of these complex metal hydrides so far.

In this brief review article, some results of our recent studies on Li- and Mg-alanates, zinc borohydride as well as thermodynamic evaluation on destabilization of high temperature hydrides such as MgH_2 and $LiBH_4$ will be described.

2. Alanates

A group of alanates (aluminum hydrides), such as $NaAlH_4$, has high hydrogen storage capacity (> 5 %) and relatively low decomposition temperature (< 150 ℃) compared to binary metal hydrides such as LiH and MgH_2 (> 300 ℃), although it was generally believed that these complex metal hydrides are difficult to operate reversibly in the dehydrogenation/hydrogenation cycle. However, Bogdanovic and Schwickardi [1] found in 1997 that $NaAlH_4$ can be made reversible under practical hydrogen pressure (< 150 bar) by “doping” with Ti-containing compounds. Since then, other alanates such as $LiAlH_4$ and $Mg(AlH_4)_2$ have been also studied as promising hydrogen storage materials.

2.1. Li_3AlH_6

The theoretical hydrogen capacity of $LiAlH_4$ is 7.9 % and its thermal decomposition behaviour is known to be similar to that of $NaAlH_4$. It seems, however, that the hydrogen pressure needed for rehydrogenation of Li_3AlH_6 to $LiAlH_4$ is estimated to be an order of 10^4 bar which is beyond practical limit [2]. It is, therefore, natural to start with Li_3AlH_6 (5.6 % theoretical capacity) as the decomposition reaction of Li_3AlH_6 into a mixture of LiH, Al and H_2 is known to be endothermic [3].

X-ray diffraction (XRD) patterns of Li_3AlH_6 catalyzed with $TiAl_3$ and $TiCl_3$ are presented in Fig. 1. It seems that $TiAl_3$ is stable in Li_3AlH_6 without any reaction or transformation (Fig. 1a), although most of $TiAl_3$ peaks except for (220) overlap with those of Li_3AlH_6. It is believed that $TiCl_3$ dispersed into Li_3AlH_6 reacts with part of Li_3AlH_6 and forms LiCl and $TiAl_3$ as reaction products. While the formation of LiCl is clear as shown in the XRD pattern (Fig. 1b), the formation of $TiAl_3$ is not evident with a small amount of $TiCl_3$. This is presumably because the crystallite size of $TiAl_3$ in situ formed in Li_3AlH_6 is too small to identify with XRD. However, we observed the obvious formation of $TiAl_3$ in Li_3AlH_6 catalyzed with 17 mol% $TiCl_3$ using XRD [4].

TG curves show the amount of released hydrogen as well as the dehydrogenation temperature region (Fig. 2). Li_3AlH_6 without catalysts releases about 4.8 % during dehydrogenation, which is lower than the theoretical hydrogen storage capacity 5.6 % due to the low purity of raw materials and the partial decomposition of Li_3AlH_6 during mechanochemical preparation. It is noted that Li_3AlH_6 catalyzed with $TiAl_3$ releases larger amount of hydrogen (4.5 %) than $TiCl_3$ (4.0 %) as expected. This is because $TiCl_3$ decomposes part of Li_3AlH_6 during milling for dispersion before dehydrogenation and thus decreases the hydrogen storage capacity of Li_3AlH_6. Therefore, it will be favorable to add $TiAl_3$ instead of $TiCl_3$ into alanates in order to minimize the loss in hydrogen storage capacity.

2.2. $Mg(AlH_4)_2$

Instead of using a solvent as ion carrier to promote chemical reaction, a ball milling method [5] was adopted in the present study to induce intimate physical contact between reactants without the help of any solvent. Although this mechanochemical reaction proceeds through a solid-state reaction at room temperature, the enhanced local reactivity by mechanical activation allows the reaction product to form very quickly. It was, therefore, possible to prepare solvent-free magnesium alanate by this mechanochemical reaction.

Fig. 3 shows the XRD pattern of $Mg(AlH_4)_2$ + NaCl formed after milling for 1 h. It consists of $Mg(AlH_4)_2$ and by-product NaCl and no reactant was observed. The diffraction peaks from $Mg(AlH_4)_2$ as shown in Fig. 1 match very well with the literature data [6]. The thermal decomposition characteristics of $Mg(AlH_4)_2$ (+NaCl) was investigated by thermogravimetry (TG)/mass spectrometry (MS) and the result is given in Fig. 4. The first decomposition reaction starts at about 115 ℃ and completes at 150 ℃. The second decomposition starts at about 240 ℃ and completes at 290 ℃. Both decomposition reactions accompany hydrogen evolution and no other vapor phase was detected by MS. The weight losses in the first and second decomposition steps are 2.8 % and 1.0 %, respectively, and the measured total weight

loss of 3.8 % matches very well with the theoretical one of 3.9 %.

The result of differential scanning calorimetry (DSC) measurement is shown in Fig. 5. An exothermic peak at about 130 ℃ was clearly detected and a larger endothermic peak around 285 ℃ was also observed. Both the first exothermic and second endothermic peak temperatures match well with the first and second weight loss steps, respectively. It is, therefore, concluded that the first exothermic reaction corresponds to the decomposition of $Mg(AlH_4)_2$ and the second endothermic peak to the decomposition of MgH_2. We have also calculated the enthalpy change at 0 K by ab-initio calculations within a density functional theory (DFT)-generalized gradient approximation (GGA) framework using VASP software [7]. The atomic positions and the cell parameters, including the cell volume, were optimized by minimizing the forces and stresses. A 6×6×6 Monkhorst-Pack *k*-point mesh was used for sampling the Brillouin zone. A kinetic energy cutoff of 450 eV was chosen for the plane wave basis set to ensure convergence. The calculated enthalpy change at 0K is −20.4 kJ/mol and it agrees well with the estimated value −18 kJ/mol from the DSC measurement between 115 and 140 ℃. Setten [8] also calculated the enthalpy of the first decomposition reaction at 0 K by the same method as ours recently and obtained −16.4 kJ/mol. It is, therefore, concluded that the first decomposition reaction of $Mg(AlH_4)_2$ is indeed exothermic.

As the first decomposition of $Mg(AlH_4)_2$ is exothermic, i.e., the enthalpy change is negative, and the entropy change is roughly estimated to be around +100 J/K/mol of H_2, which is a typical value in metal hydride formation reaction, the reverse reaction to form $Mg(AlH_4)_2$ from MgH_2, Al and H_2 is not likely to occur because the free energy change of the reverse hydrogenation reaction will be positive unless the hydrogenation pressure P_{H2} is extremely high (> 10^4 bar). Moreover, the decomposition of Al_3Mg_2 to free Al and Mg will not proceed, as ΔG of the reaction is positive below the melting temperature of Al_3Mg_2. From these thermodynamic evaluations, it is concluded that $Mg(AlH_4)_2$ is not suitable for reversible hydrogen storage materials, although it has high theoretical hydrogen capacity (9.3 %) and relatively low decomposition temperature (< 150 ℃).

From the above results, it is proposed that $Mg(AlH_4)_2$ decomposes in two steps as follows:

$$Mg(AlH_4)_2 \rightarrow MgH_2 + 2Al + 3H_2(\uparrow) \qquad (115–150\ ℃)$$

$$MgH_2 + 2Al \rightarrow 1/2Al_3Mg_2 + 12Al + H_2(\uparrow) \qquad (240–290\ ℃)$$

The decomposition temperature of MgH_2 formed after the first decomposition step was significantly lower than that of the pure MgH_2 that was measured at same condition. It is believed that active Al formed after the first decomposition step destabilized MgH_2 to produce

more stable Al_3Mg_2. In fact, we calculated the phase stability of the H_2, Mg, Al, MgH_2, Al_3Mg_2 using SGTE substance and solution databases that are incorporated into Thermo-Calc software [9] under 1 bar of hydrogen. Al_3Mg_2 +H_2 become more stable than MgH_2 +Al above 243 ℃, which agrees with the experimental data obtained in the present study.

3. Zinc borohydride

$Zn(BH_4)_2$ belongs to complex metal hydrides which are represented as $M_x(BH_4)_y$ (M = Li, Na, K, Rb, Cs, Zn, etc.), in which there is current interest as potential hydrogen storage materials [10,11]. It has high theoretical hydrogen capacity (8.5 %) and is reported to have low decomposition temperature (50–120 ℃) [12]. It can be prepared by metathesis reaction between $NaBH_4$ and $ZnCl_2$ in an appropriate solvent such as diethyl ether [13]. It is, however, difficult to remove solvent completely without causing decomposition of $Zn(BH_4)_2$ itself. Therefore, the thermal decomposition behavior of adduct-free $Zn(BH_4)_2$ could not be properly investigated in the past. In this paper, we have investigated the stability and thermal decomposition behavior of $Zn(BH_4)_2$ prepared by mechnochemical reaction between $NaBH_4$ and $ZnCl_2$ at room temperature without using any solvent.

The XRD pattern of the product powder after ball milling for 30 min is presented in Fig. 6. Although information on the crystal structure of $Zn(BH_4)_2$ is not available at present, the remaining peaks, after excluding NaCl peaks, were found to match quite well with those of the previous studies [14]. Neither $ZnCl_2$ nor $NaBH_4$ peaks were observed, which indicates that the following reaction is completed after milling for 30 minutes.

$$ZnCl_2 + 2NaBH_4 \rightarrow Zn(BH_4)_2 + 2NaCl \quad (1)$$

The result of TG/MS measurement of $Zn(BH_4)_2$(+NaCl) is presented in Fig. 7a. The decomposition reaction started at about 85 ℃ and completed at about 140 ℃. It was accompanied by the evolution of hydrogen. As soon as the decomposition reaction started, a sharp endothermic peak was recorded between 85 and 105 ℃ in DSC curve as shown in Fig. 7b. This peak is attributed to the melting of $Zn(BH_4)_2$. In fact, the melting phenomenon was visually confirmed by heating the sample contained in an argon filled vial under a stereoscopic microscope. A broad endothermic peak due to relatively slow decomposition reaction was also detected between 85 and 140 ℃ and it matches well with the weight loss curve.

As the reaction product after milling contains 2 mol of NaCl for every 1 mol of $Zn(BH_4)_2$, the total weight loss after the completion of dehydrogenation reaction is expected to be 3.8 % rather than 8.5 % of pure $Zn(BH_4)_2$ if hydrogen is the only evolving gas during thermal

decomposition. However, the measured weight loss was 12.1 %, which is much higher than the expected 3.8 %. After careful examination of MS spectrum, it was confirmed that a significant amount of diborane B_2H_6 [15] was also produced as shown in Fig. 8. The calculated boron content in the $Zn(BH_4)_2$(+NaCl) mixture is 10.2% and the predicted total weight loss (hydrogen + diborane) is, therefore, 14.0 % which is slightly higher than the measured value. It was later confirmed by ICP-AES that the residual boron content in the final decomposition product was 0.8 %. Considering a possibility of partial decomposition of $Zn(BH_4)_2$ during mechanochemical reaction process, it is concluded that the measured weight loss agrees with the calculated one rather well.

The XRD pattern of the $Zn(BH_4)_2$(+NaCl) sample heated at 150 ℃ for 3 days is presented in Fig. 9. Metal Zn was observed together with NaCl, but the existence of either crystalline or amorphous B could not be determined in the XRD pattern as the amount of boron is too small to be detected by XRD. In addition, a considerable amount of free Zn was observed in the XRD pattern of the as milled sample stored in a sealed vial inside the globe box for one week at room temperature. This clearly indicates that $Zn(BH_4)_2$ is unstable even at room temperature [16].

From the above results, the thermal decomposition of $Zn(BH_4)_2$ can be described as follows:

$$Zn(BH_4)_2\ (\text{solid}) \rightarrow Zn(BH_4)_2\ (\text{liquid})$$
$$Zn(BH_4)_2\ (\text{solid or liquid}) \rightarrow Zn + B_2H_6 + H_2$$

4. Destabilization of high temperature metal hydrides: thermodynamics

4.1. MgH_2-Si system

MgH_2 is considered to be one of the promising hydrogen storage materials for many applications due to its high storage capacity and excellent reversibility, not to mention its low cost. The problem of slow hydrogenation kinetics has recently been solved by adopting appropriate catalysts [17–19] with the help of mechanical milling. The high decomposition temperature is the last major obstacle to be removed before MgH_2 becomes a serious contender versus high pressure tank storage technology for on-board applications. There are some light elements that react with MgH_2 to form stable intermetallic compounds, and Mg_2Si is among them. It does not reduce the theoretical hydrogen storage capacity, from 7.6 % for pure MgH_2 to 5.0 % for $2MgH_2$ + Si mixture, as much as Mg_2Ni does. The results of the thermodynamic calculations are given in Table 1 and Fig. 10 [20]. It is estimated that it decomposes even at room temperature for 1 bar hydrogen, and the equilibrium hydrogen pressure reaches 100 bar at about 130 ℃. In fact, Vajo et al. [21] have recently tried to promote the reaction between MgH_2 and Si by high energy ball milling with and without a catalyst, but could not observe any

reaction up to the decomposition temperature of pure MgH_2 (285 ℃), although the hydrogen pressure at 300 ℃ was higher than 7 bar. Reversible hydrogenation of Mg_2Si to a mixture of MgH_2 and Si was not observed either at 150 ℃ under 100 bar of hydrogen. However, they reported that an uptake of 0.8 % hydrogen could be achieved by high energy ball milling pure Mg_2Si in 50 bar of hydrogen for 48 hours. They suggested that a mechanical activation might have helped to overcome the kinetic barriers to hydrogenation at low temperatures.

The diffusion of Si at low temperatures is expected to be very slow and will almost certainly control the reaction between MgH_2 and Si. Therefore, the particle size of the reactants, particularly Si, needs to be reduced as much as possible and the formation of surface oxide on Si particles should be avoided as much as possible in order to lower the kinetic barriers. For the hydrogenation of Mg_2Si, adding a proper catalyst would help a lot to render the dissociation of hydrogen molecules into hydrogen atoms possible. Nevertheless, it is unlikely that the actual decomposition temperature would be reduced to room temperature unless MgH_2 and Si are mixed almost on a molecular level.

4.2. $LiBH_4$-MgH_2 system

Lithium borohydride $LiBH_4$ is an ionic, white, crystalline solid that is sensitive to moisture but not to oxygen. Its crystal structure is orthorhombic (space group *Pnma*) at room temperature but it transforms into hexagonal (space group $P6_3mc$) at about 110 ℃. It melts at 278 ℃ and decomposes slowly above 380℃ according to the following reaction [22]:

$$LiBH_4 \rightarrow LiH + B + 1.5H_2.$$

The amount of hydrogen expected to be released by this reaction is 13.9 %. It has been reported that the decomposition temperature of $LiBH_4$ could be lowered to about 200 ℃ when SiO_2 is added as a catalyst [11]. Instead of adopting the “alloying” option, we have further extended the idea of destabilization by exploiting a chemical reaction with light metals or even metal hydrides such as Al and MgH_2, which produces more stable metal borides. The $LiBH_4 + MgH_2$ system is expected to undergo the following single step reaction which generates 11.5 % hydrogen:

$$2LiBH_4 + MgH_2 \rightarrow 2LiH + MgB_2 + 4H_2$$

The result of thermodynamic calculation is also given in Table 1 and Fig. 10. The reaction with MgH_2 is expected to reduce the decomposition temperature of $LiBH_4$ from about 400 ℃ to

approximately 170 ℃ according to the present thermodynamic calculation. A preliminary result of the recent experiment by Vajo et al. [23] does not agree, however, with that of the present thermodynamic calculation (see Fig. 4 in Ref. [23]), although they did confirm that the hydrogen pressure of 4.5 bar could be obtained at 315 ℃ with the help of $TiCl_3$ as a catalyst. They also reported that the reverse hydrogenation reaction did occur under a hydrogen pressure of 100 bar between 230 and 350 ℃.

Both $LiBH_4$ and MgH_2 are quite stable compounds, and even comparatively less stable MgH_2 decomposes at 170 ℃ to produce a hydrogen pressure of only 0.01 bar and Mg. Therefore, homogeneous mixing at approaching molecular levels may be required to alleviate the kinetic energy barrier of the reaction significantly, as well as to reduce the diffusion length of both the reactants. The selection of a more effective catalyst and the proper use of it may also help to initiate the decomposition reaction at lower temperatures.

5. Conclusions

Although solid hydrogen storage utilizing conventional metallic hydrides has certain advantages of compactness and safety against high pressure compression tank system, most of them have quite low gravimetric density of less than 2 %. Recent studies on some complex metal hydrides, such as $NaAlH_4$ and $LiNH_2$, have shown that more than 4 % of hydrogen can be reversibly stored at temperatures below 150 ℃ and under about 100 bar of H_2. More experimental and theoretical studies on many less known complex metal hydrides have to be intensively carried out in order to find a promising material for reversible on board hydrogen storage applications.

Acknowledgements

Part of this work has been financially supported by the Hydrogen Energy R&D Center under the 21st Century Frontier R&D Program and by Korea Science and Engineering Foundation under the International Cooperative Research Program of the Ministry of Science and Technology, Republic of Korea.

References

1. B. Bogdanović, M. Schwickardi, J. Alloys Compd. 253, 1 (1997).
2. J.-W. Jang, J.-H. Shim, Y.W. Cho, B.-J. Lee, J. Alloys Comd., (2006), in press.
3. J.-H. Shim, G.-J. Lee, Y.W. Cho, J. Alloys Compd., (2006), in press.
4. J.-H. Shim, G.-J. Lee, Y.W. Cho, J. Alloys Compd., (2006), in press.
5. C. Suryanarayana, Prog. Mater. Sci. 46, 1 (2001).

6. A. Fossdal, H.W. Brinks, M. Fichtner, B.C. Hauback, J. Alloys Compd. 387, 47 (2005).
7. G. Kresse, J. Furthmüller, Comput. Mater. Sci. 6, 15 (1996).
8. M. Setten, G. Wijs, V. Popa, G. Brocks, http://arxiv.org/abs/condmat/ 0505623.
9. http://www.thermocalc.se
10. G. Tenaudin, S. Gomes, H. Hagemann, L. Keller, K. Yvon, J. Alloys Compd. 375, 98 (2004).
11. A. Zuttel, S. Rentsch, P. Fischer, P. Wenger, P. Sudan, Ph. Mauron, Ch. Emmenegger, J. Alloys Compd. 356, 515 (2003).
12. W. Grochala, P.P. Edwards, Chem. Rev. 104, 1283 (2004).
13. T.J. Marks, J.R. Kolb, Chem. Rev. 77, 263 (1977).
14. K.G. Myakishev, I.I. Gorbacheva, O.G. Potapova, V.V. volkov, Seriya Khimisheskikh Wauk. 4, 55 (1989).
15. E. McLaughlin, T.E. Ong, R.W. Rozett, J. Phys. Chem. 75, 3106 (1971).
16. K.M. Mackay, Hydrogen Compounds of the Metallic elements, E&F.N. Spon Ltd., London, 1966, p. 1.
17. A. Zaluska, L. Zaluski, J.O. Ström-Olsen, J. Alloys Compd. 289, 197 (1999).
18. G. Liang, J. Hout, S. Boily, A. Van Neste, R. Schulz, J. Alloys Compd. 291, 295 (1999).
19. W. Oelerich, T. Klassen, R. Bormann, J. Alloys Compd. 315, 237 (2001).
20. Y.W. Cho, J.-H. Shim, B.-J. Lee, CALPHAD 30, 65 (2006).
21. J.J. Vajo, F. Mertens, C.C. Ahn, R.C. Bowman Jr., B. Fultz, J. Phys. Chem. B 108, 13977 (2004).
22. A. Züttel, P. Wengner, S. Rentsch, P. Sudan, Ph. Mauron, Ch. Emmenegger, J. Power Sources 118, 1 (2003).
23. J.J. Vajo, S. Skeith, F. Mertens, J. Phys. Chem. B 109, 3719 (2005).

Table 1. Calculated decomposition temperatures of various chemical reactions for the destabilization of metal hydrides.

Reactions	Theoretical hydrogen storage capacity	Calculated decomposition temperature of pure MH/MBH_4 (1bar H_2)	Calculated destabilized temperature. (1bar H_2)
$2MgH_2 + Si \rightarrow Mg_2Si + 2H_2$	5.0 wt%	288 ^oC (MgH_2)	23 ^oC
$2MgH_2 + 3Al \rightarrow Al_3Mg_2 + 2H_2$	3.0 wt%	288 ^oC (MgH_2)	241 ^oC
$12LiH + 7Si \rightarrow Li_{12}Si_7 + 6H_2$	5.0 wt%	874 ^oC (LiH)	485 ^oC
$7LiH + 3Si \rightarrow Li_7Si_3 + 3.5H_2$	4.1 wt%	874 ^oC (LiH)	502 ^oC
$2LiBH_4 + MgH_2 \rightarrow 2LiH + MgB_2 + 4H_2$	11.5 wt%	403 ^oC ($LiBH_4$)	165 ^oC
$2LiBH_4 + Al \rightarrow 2LiH + AlB_2 + 3H_2$	8.6 wt%	403 ^oC ($LiBH_4$)	188 ^oC
$2NaBH_4 + Al \rightarrow 2NaH + AlB_2 + 3H_2$	5.8 wt%	602 ^oC ($NaBH_4$)	459 ^oC

Figure captions

Fig. 1. XRD patterns of Li_3AlH_6 with (a) $TiAl_3$ and (b) $TiCl_3$.

Fig. 2. TG curves of Li_3AlH_6 with and without catalysts.

Fig. 3. XRD pattern of $Mg(AlH_4)_2$(+NaCl) prepared by milling $NaAlH_4$+$MgCl_2$ for 1 hour. Open circle and solid square indicate $Mg(AlH_4)_2$ and NaCl, respectively.

Fig. 4. TG and hydrogen MS curves of $Mg(AlH_4)_2$(+NaCl) prepared by milling Na $NaAlH_4$+$MgCl_2$ for 1 hour. The straight and dash-dot lines indicate TG and MS curves, respectively.

Fig. 5. DSC curve of $Mg(AlH_4)_2$(+NaCl) prepared by milling Na $NaAlH_4$+$MgCl_2$ for 1 hour.

Fig. 6. XRD patterns of $Zn(BH_4)_2$(+NaCl). The asterisk indicates a diffraction peak of NaCl.

Fig. 7. (a) TG and hydrogen MS curves of $Zn(BH_4)_2$(+NaCl), (b) TG and DSC curves of $Zn(BH_4)_2$(+NaCl).

Fig. 8. (a) TG and diborane (B_2H_6) MS curves and (b) DSC and diborane (B2H6) MS curves of $Zn(BH_4)_2$(+NaCl).

Fig. 9. XRD pattern of $Zn(BH_4)_2$(+NaCl) after heating for 3 days at 150 ℃. The asterisk indicates a diffraction peak of NaCl.

Fig. 10. Calculated van't Hoff plots of various chemical reactions for destabilization of metal hydrides.

Figure 1

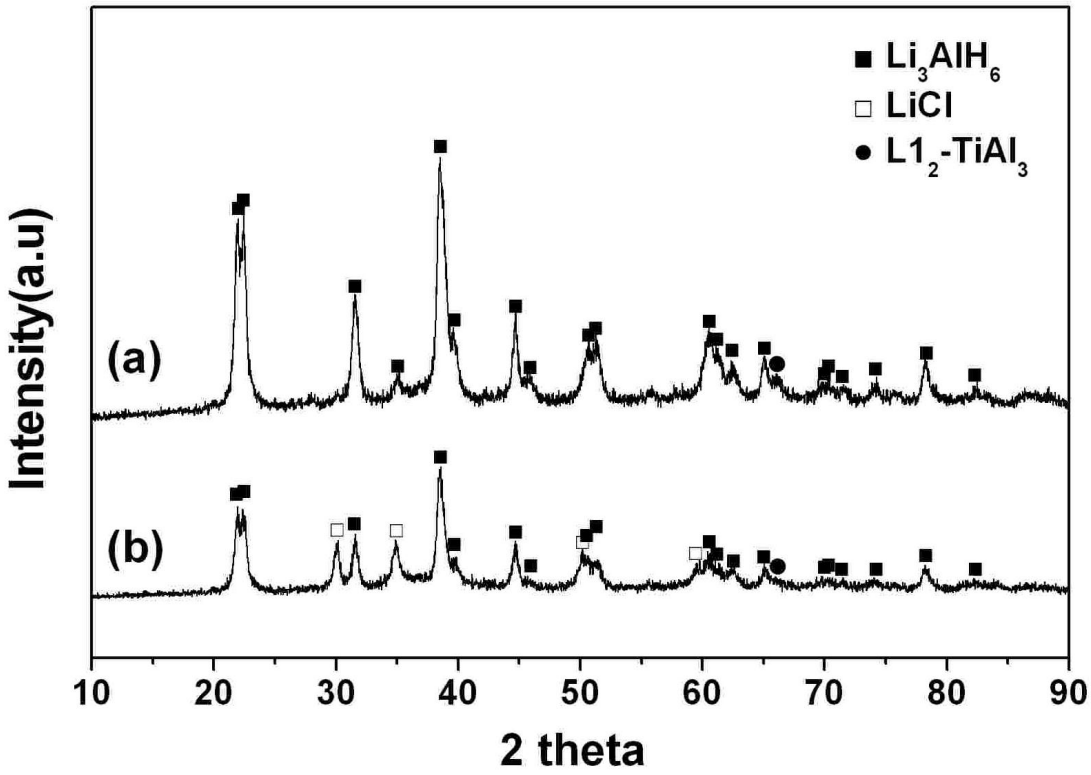
■ Li_3AlH_6
□ LiCl
● $L1_2$-$TiAl_3$
(a)
(b)
Intensity(a.u)
10
20
30
40
50
60
70
80
90
2 theta

Figure 2

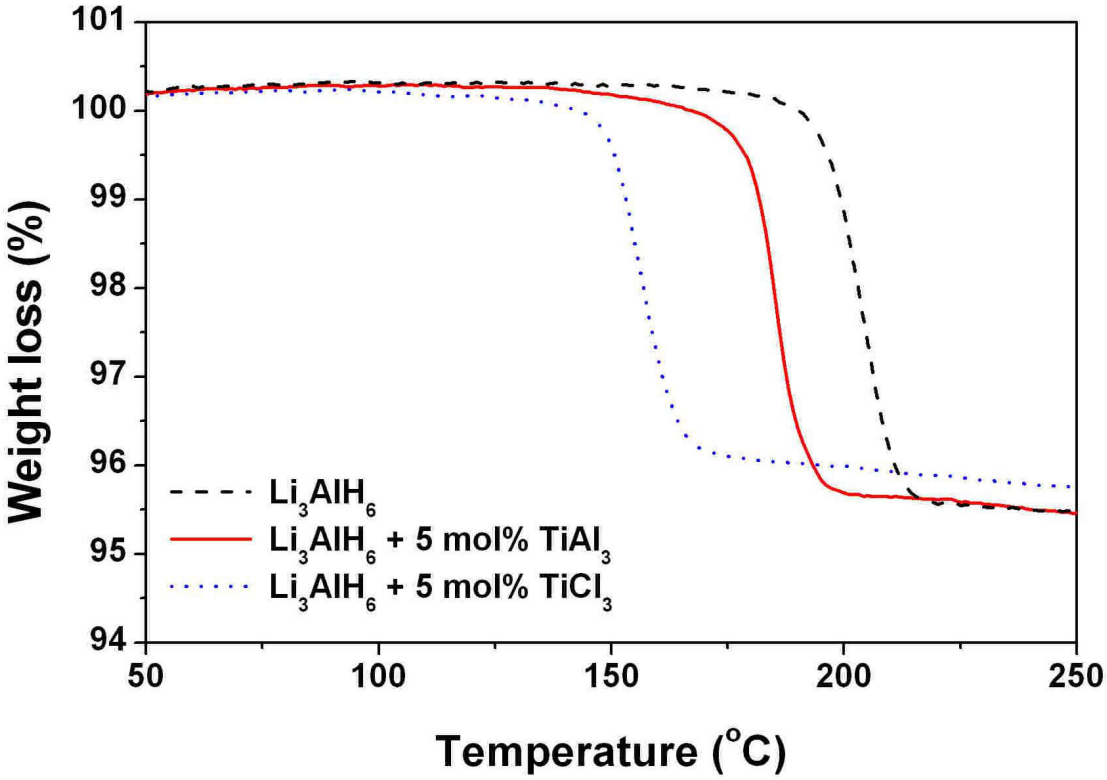
Weight loss (%)
101
100
99
98
97
96
95
94
50
100
150
200
250
Temperature (°C)
Li3AlH6
Li3AlH6 + 5 mol% TiAl3
Li3AlH6 + 5 mol% TiCl3

Figure 3

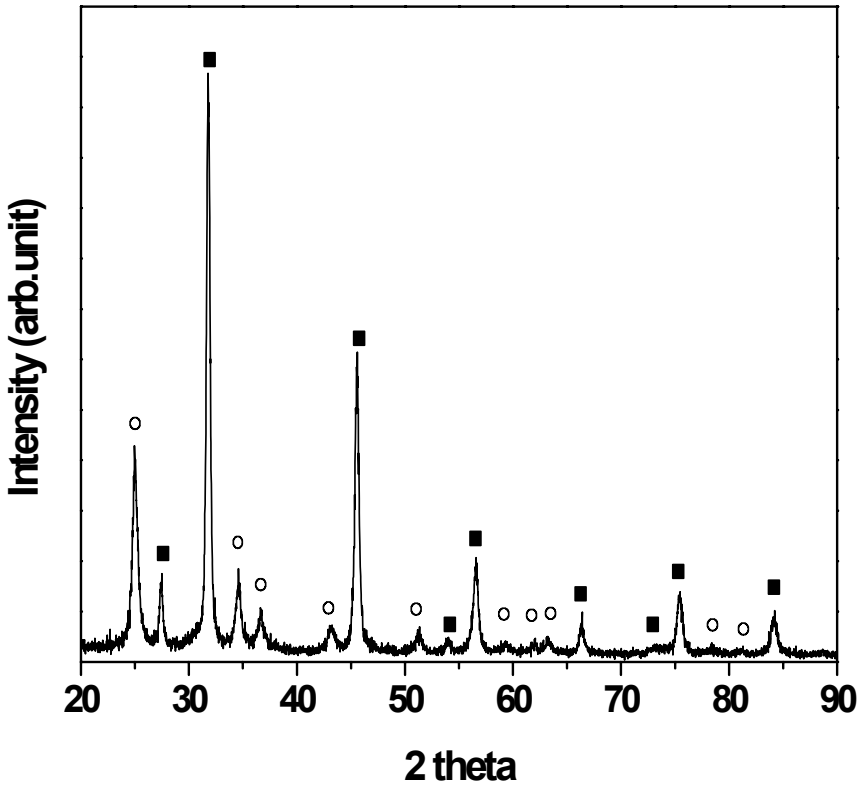

Figure 4

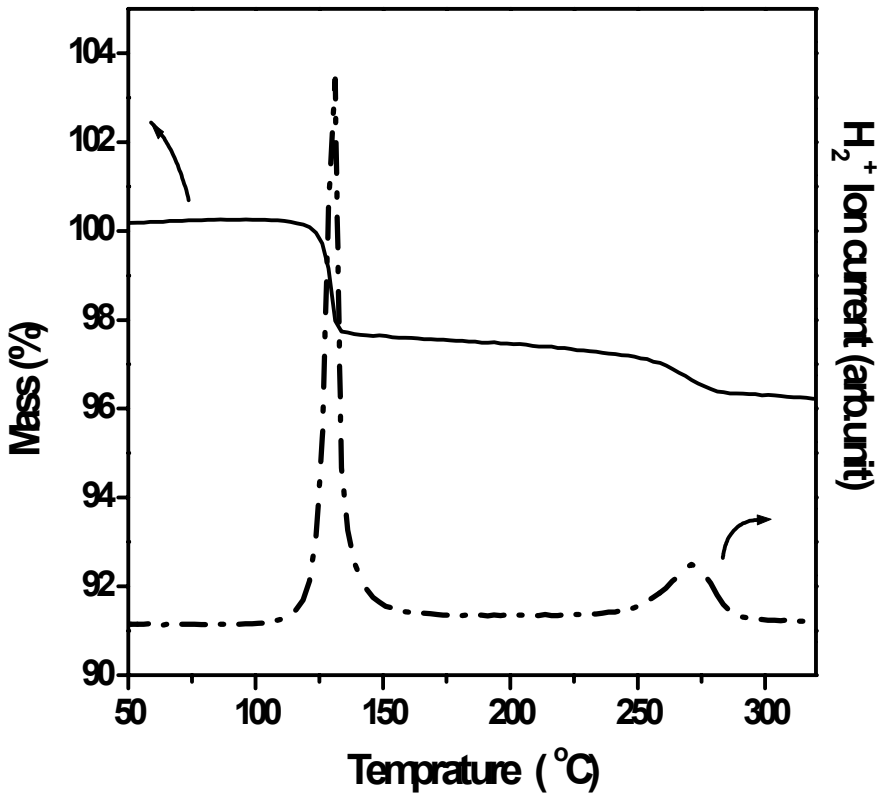
104
102
100
98
96
94
92
90
Mass (%)
50
100
150
200
250
300
Temprature (°C)
H2+ Ion current (arb.unit)

Figure 5

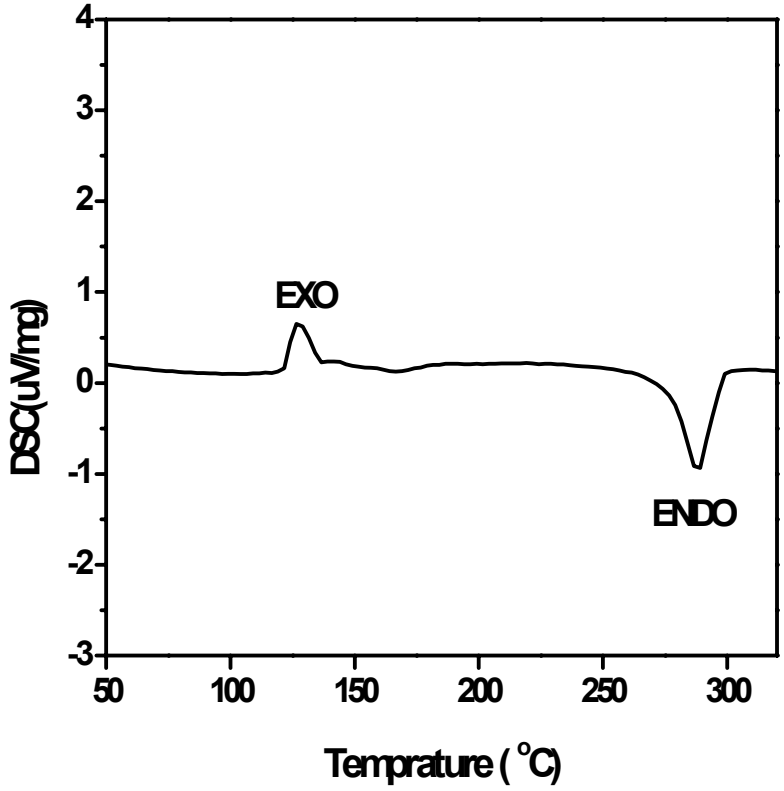
4
3
2
1
0
-1
-2
-3
DSC(uV/mg)
EXO
ENDO
50
100
150
200
250
300
Temprature (°C)

Figure 6

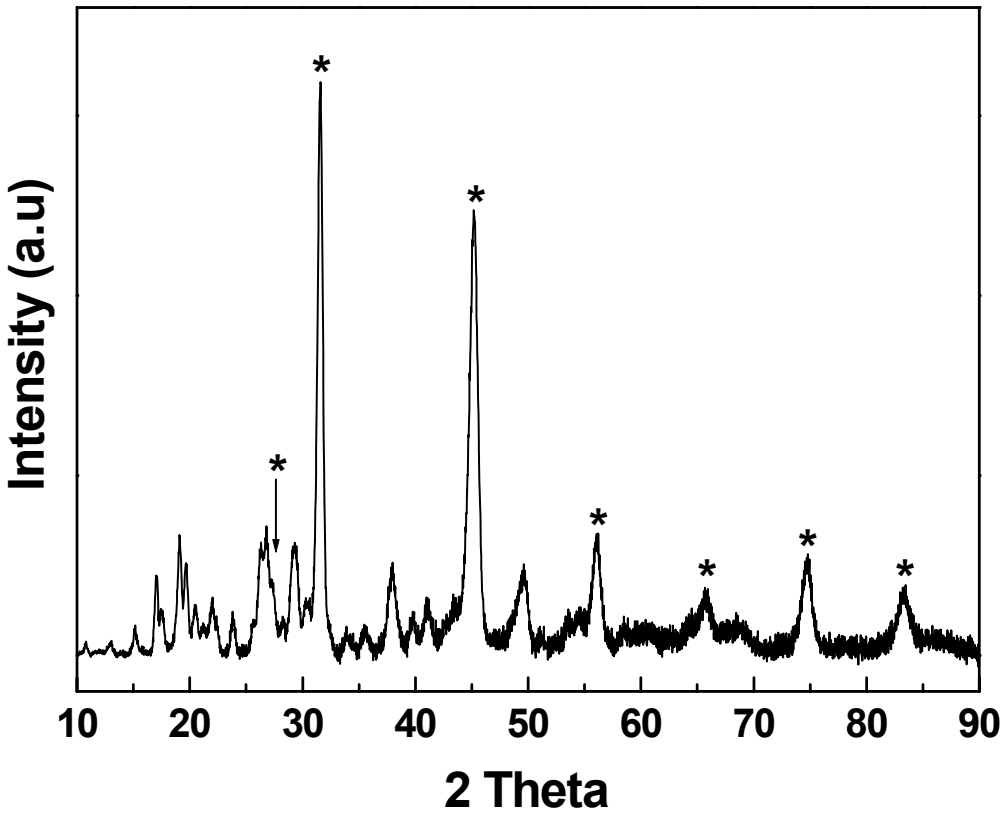

Figure 7

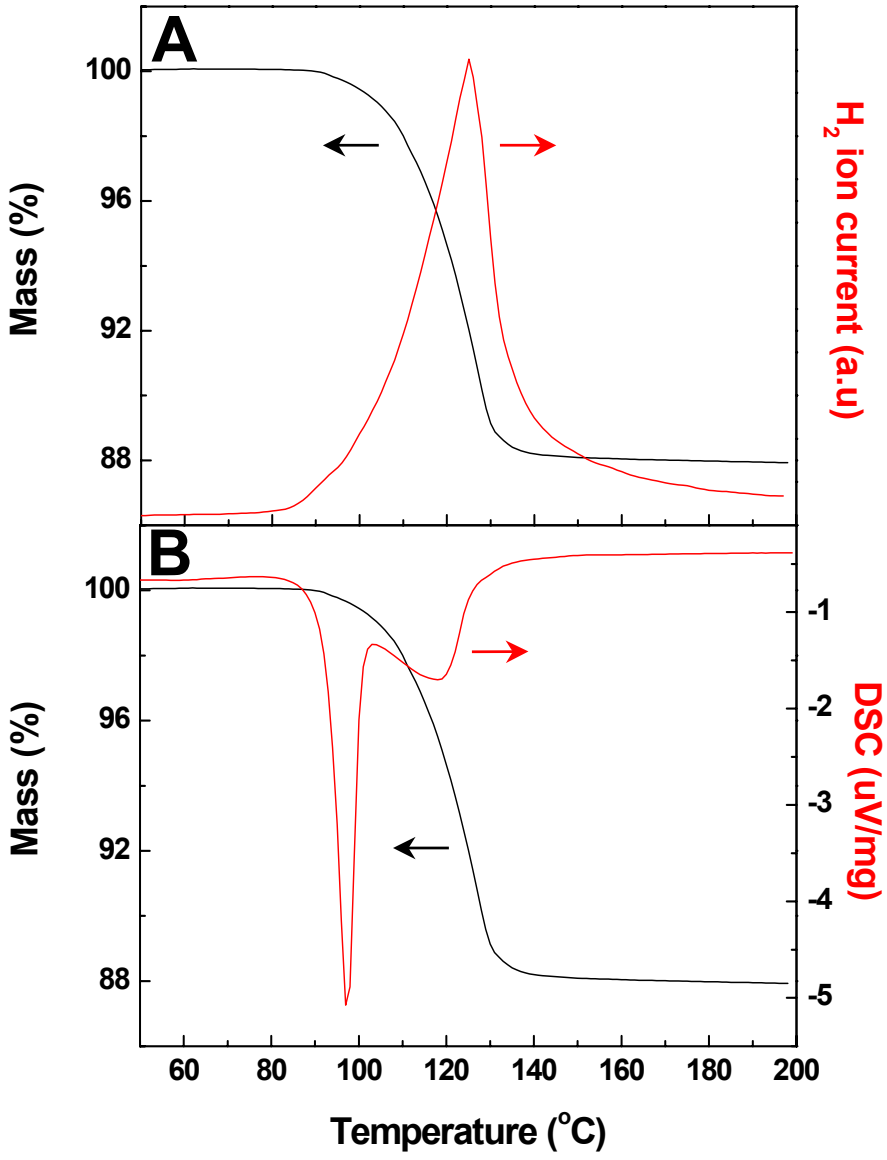
A
B
100
96
92
88
Mass (%)
H2 ion current (a.u)
-1
-2
-3
-4
-5
DSC (uV/mg)
60
80
100
120
140
160
180
200
Temperature (°C)

Figure 8

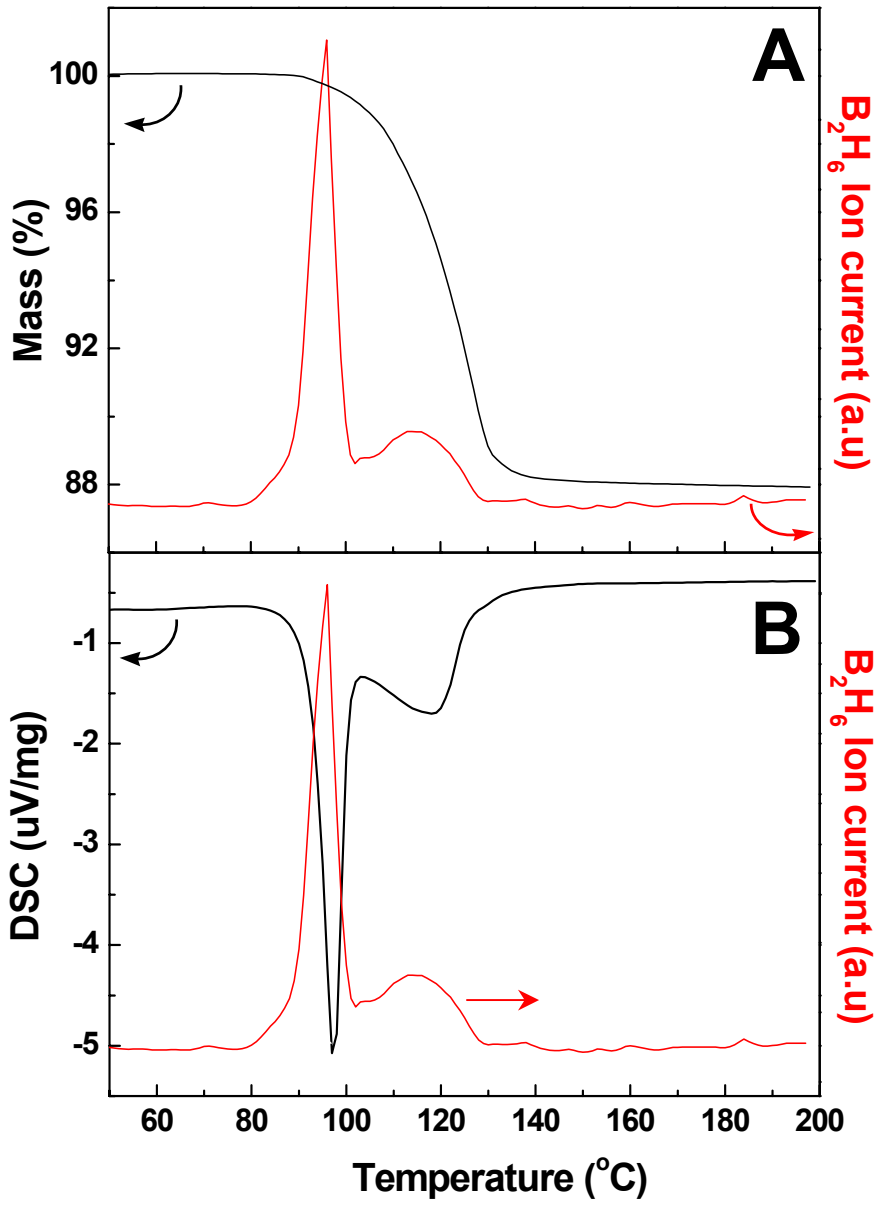
A
B
100
96
92
88
Mass (%)
B_2H_6 Ion current (a.u)
-1
-2
-3
-4
-5
DSC (uV/mg)
B_2H_6 Ion current (a.u)
60
80
100
120
140
160
180
200
Temperature (°C)

Figure 9

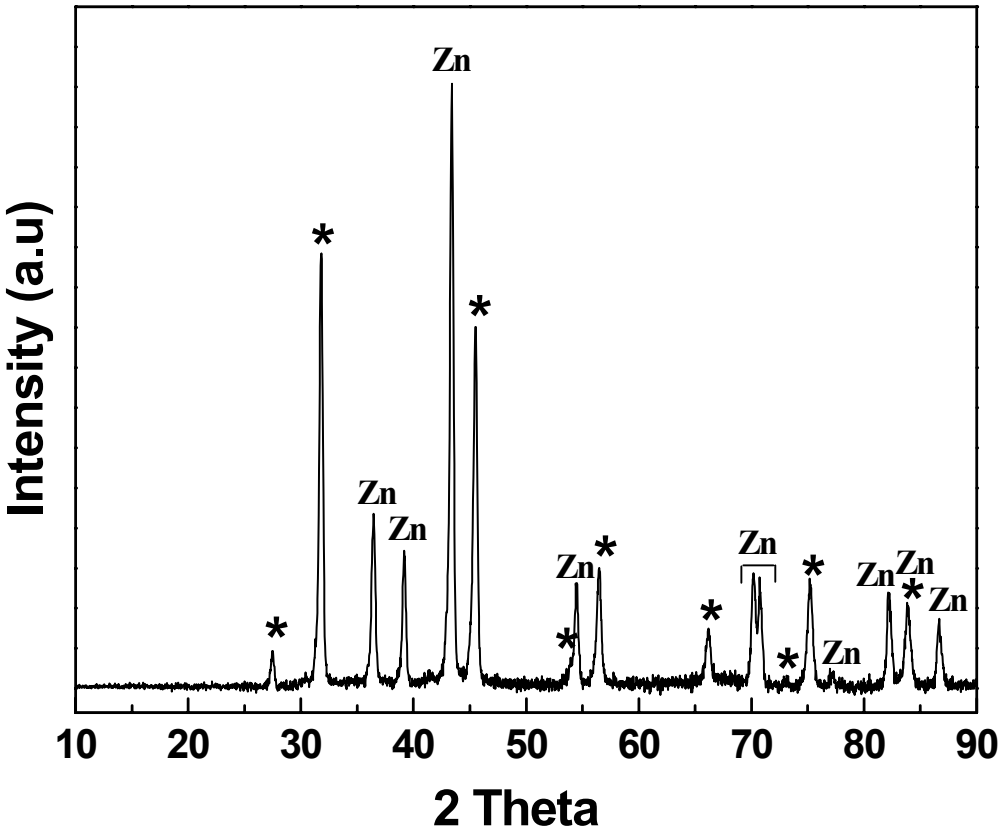

Figure 10

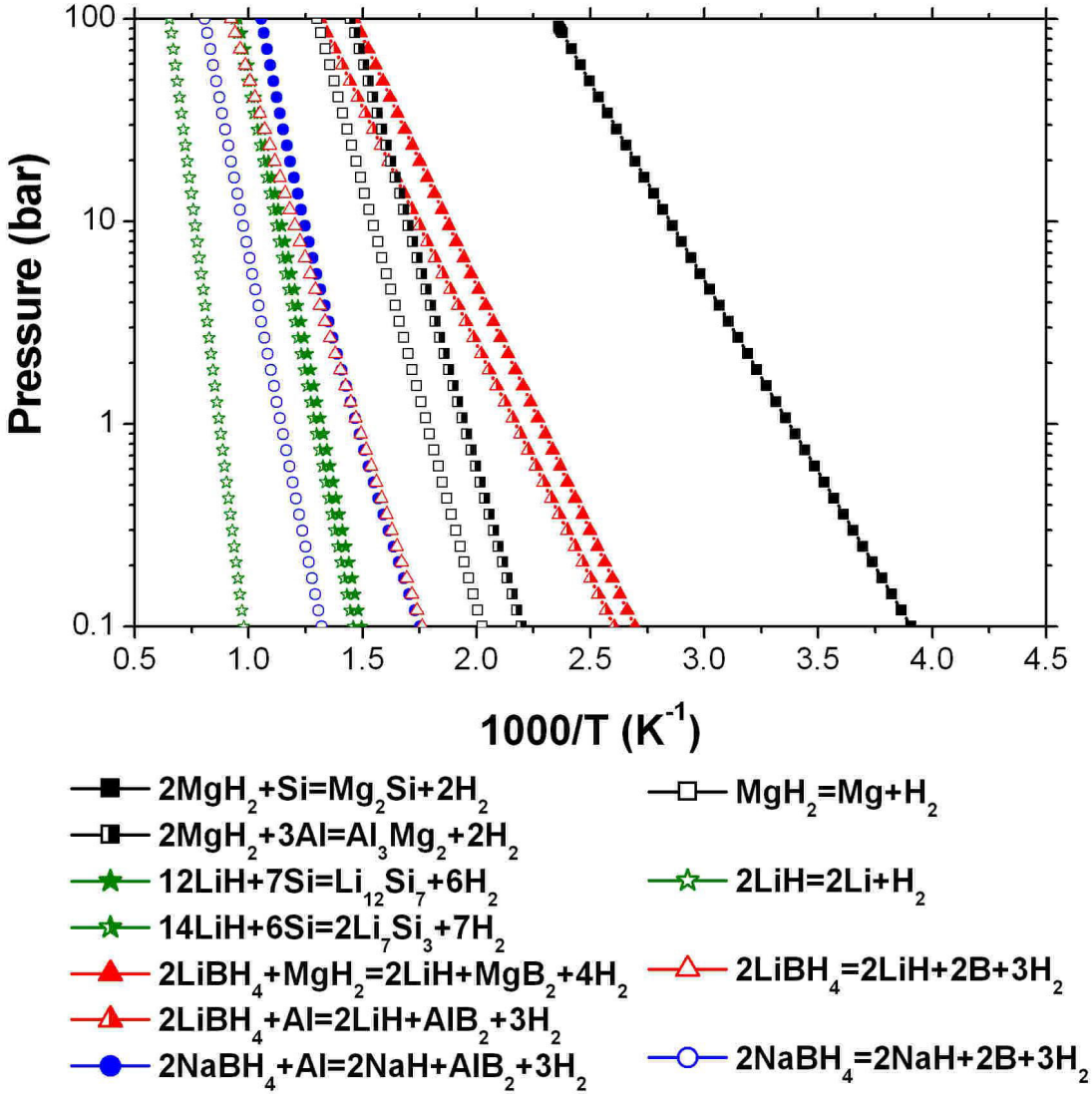
Pressure (bar)
100
10
1
0.1
0.5
1.0
1.5
2.0
2.5
3.0
3.5
4.0
4.5
1000/T (K-1)
2MgH2+Si=Mg2Si+2H2
MgH2=Mg+H2
2MgH2+3Al=Al3Mg2+2H2
12LiH+7Si=Li12Si7+6H2
2LiH=2Li+H2
14LiH+6Si=2Li7Si3+7H2
2LiBH4+MgH2=2LiH+MgB2+4H2
2LiBH4=2LiH+2B+3H2
2LiBH4+Al=2LiH+AlB2+3H2
2NaBH4+Al=2NaH+AlB2+3H2
2NaBH4=2NaH+2B+3H2